A BLUNTED CONE IN A SUPERSONIC HIGH-ENTHALPY NONEQUILIBRIUM SUPERSONIC AIR FLOW

V I. Sakharov[1], V.V. Shtapov[2], E.B. Vasilevskiy*[3], B.E. Zhestkov*[4]*

**[1] Head of laboratory of Institute*

Mechanics at the Lomonosov Moscow State University, 119192, Moscow, Russia.,

**[2] Engineer, **[3] Head of division, **[4] Head of laboratory*

**[2-4] Central Aerohydrodynamic Institute, 140180, Zhukovsky str.1, Zhukovsky, Moscow region, Russia

Abstract

Calculation and experimental study was conducted with the flow, heat flux and pressure distribution over the front and side surfaces of a blunt cone in a non-equilibrium high-enthalpy (h_0 = 25 MJ/kg) supersonic (M = 4) air flow. Experiments were performed in wind tunnel (WT) VAT-104, TsAGI. The nose part of the model with a small-radius nose R_w = 10 mm and half angle θ = 10° was inside the "Mach cone" of the underexpanded jet flowing out from the WT nozzle. Numerical and experimental results are in agreement.

1. Introduction

Simulation of thermo-chemical interaction between high-enthalpy flows of air and other gases and heat-protective materials (HPM) in high-enthalpy wind tunnels (WT) for flight conditions of bodies with hypersonic speeds in atmosphere of the Earth, Mars, and other planets is among key problems of air thermo-dynamics [1].

Inductive (electrodeless) plasmatorches which produce high-enthalpy chemically pure gas flows, have a good potentiality in such simulation, particularly in respect to the thermal effect of heterogeneous catalytic reactions of atomic recombination [2-10]. Such WT are utilized, in particular, to carry out ground experimental researches of the thermal protection for the flight conditions of hypersonic aircrafts (HA) in the upper regions of the Earth atmosphere (about 60 – 100 km). These WT enable to study HPM properties such as surface catalyticity, emissivity, thermal stability in flows of various gases. Such works have been performed for many years with inductive plasmatorches in TsAGI (WT VAT-104), IPM RAS (VGU-4), TsNIIMASh, Von-Karman Institute, etc.

Plasmatorch VGU-4 (IPM RAS) of 100 kW permits having both subsonic and supersonic high-enthalpy flows of air and other gases within the wide range of stagnation temperature and pressure [2-6], whereas the wind tunnel VAT-104, TsAGI, is purposed to produce supersonic (M = 4 – 8) high-enthalpy flows. Note that the simulation of heat exchange in the inductive plasmatorch at the stagnation point for the conditions of hypersonic flights suggests, among other factors, the equality of total enthalpies and pressures on the surface of flowed bodies in the ground experiment and in the hypersonic flight [7-10]. Thus, supersonic nozzles in the WT enable to expand the area of parameters for heat exchange simulation in the ground experiment.

To analyze the experimental data, in particular the catalytic properties of modern HTM, and to transfer them in full-scale conditions of the hypersonic flight of bodies in atmosphere, it is necessary to know in detail the flows realized in the experiment, as well as physical processes taking place in the WT and on model surfaces. To solve these and other challenges of modern aerodynamic experiments, one should simulate numerically the supersonic flows of chemically reacting gases and heat exchange for specific experimental conditions, including those implemented in WT VAT-104, TsAGI [10]. Today, there is serious gap between high-level mathematical and physical models applied in hypersonic aerodynamics, and approximate models utilized for the analysis of flows in WT. Numerical simulation for subsonic and supersonic regimes was successfully fulfilled.

In a number of cases, flows in WT are more complicated in respect to the analysis of obtained experimental data than the hypersonic flows near bodies incoming into the atmosphere. The wind-tunnel gas heated in the heater up to high temperature cools down when the flow speed rises as the flow goes out through the nozzle into the working chamber. The gas temperature rises again behind the shock wave induced by the flowed body. At the same time, in the flight, the gas reaches high values only after passing the shock wave induced by the body. Consequently, the gas properties

near the model in the WT and near HA surface in the flight may differ significantly at the same values of stagnation enthalpy and pressure on the body surface.
In recent years, the flows in discharge channel of the plasmatorch VGU-4 and heater WT VAT-104 were studied in the context of Navier-Stokes equations and simplified Maxwell equations, involving chemically and thermally non-equilibrium models of the gas medium, as well as the flows in flowing-out underexpanded jets of air plasma. The study was carried out within the wide range of supersonic modes of wind tunnels: air flow rates, values of the power contributed in plasma, reverse pressures in decompression chambers, sizes of outlet cross sections and sonic and supersonic nozzles.
The technology of calculation of such flows is based on a software system of numerical integration of Navier-Stokes equations and special programs-generators which include the data bases for thermodynamic and transfer properties of individual gaseous substances (HIGHTEMP) created in the Institute of Mechanics MSU [**5**].
In the present paper, numerical investigation was done for the processes and flows in a chemically non-equilibrium model of the gas medium, in the heater and channel of WT VAT-104, TsAGI, for the air dynamics of flowing-out underexpanded high-enthalpy air jets and for the model tested in the experiments; the results are compared with the experiment.
The aim of this work was to determine the heat flux and pressure distribution over the front and side surfaces of the blunt cone in the non-equilibrium high-enthalpy $h_0 = 25$ MJ/kg supersonic (M = 4) air flow. Experimental investigations were carried out in the wind tunnel WT VAT-104 TsAGI. The front part of the model with a small-radius nose $R_w = 10$ mm and half angle $\theta = 10°$ was inside the "Mach cone" of the underexpanded jet flowing out from the WT nozzle. It is known that the disturbances occurring in the working chamber of the hypersonic WT cannot penetrate into the area inside the "Mach cone" (toward the nose part of the model): this fact facilitates interpretation of the test results in comparison with the experiments in subsonic wind tunnels.
In order to measure the heat flux distribution, heat-capacity heat-flux probes were utilized (copper inserts thermally insulated from the model body). These probes were calibrated by a standard technique on a special calibrating heat-flux facility ETGU TsAGI.
To measure the pressure distribution, pressure gages were used; they were located directly inside the model. It allowed significant reducing of the pressure measurement duration in the flow by means of utilization of short routes from a receiving orifice to the pressure gage. Short duration of the measurement (test) provided complete and repetitive safety of the model under the conditions of strong action of the heat flux on it.
A special high-speed mechanism of model introduction into the high-enthalpy flow was developed for the short-run test in the WT (the time of jet crossing is below 0.2 s).

2. Experimental equipment

2.1 Wind tunnel VAT-104

Basic elements of the wind tunnel VAT-104 are the gas heater, nozzle, working chamber, and a system of pumping-out with a vacuum capacity, figure 1. Figure 1b shows the basic schematic of the WT VAT-104.
The gas is heated with a high-frequency inductive heater which permits to have a spectrally pure high-enthalpy gas flow. The heaters of this type feature high stability and repetitive accuracy of enthalpy, total stagnation pressure and heat flux from one test to another (parameter deviation from assigned values does not exceed 3%).
The inductor is fed from the high-frequency (HF) generator VChI-4-160/1.76. The generator is of a two-loop configuration, with controlled feedback. The generator power in the anode circuit is up to $Wa = 240$ kW, oscillating power is up to $W\sim = 160$ kW, frequency $\nu = 1.76$ MHz. Standard discharge ignition is carried out in the argon medium as the discharge chamber is vacuumed to the pressure of $P_0 = 5 – 30$ Pa. Then the working gas is supplied, its flow rate and heater power are increased smoothly. The flow rate of the working gas is controlled by a throttle system, manually or automatically (a program sets the mode). Mode onset time is from 10 to 30 seconds. Various gases such as nitrogen, air, argon, argon-oxygen mixture, etc. can be used as the working substance. This time, air was used.
The plasmatorch heats the working gas up to the temperature of $T_0 = 5{,}000 – 8{,}000$°C, (stagnation enthalpy is $i_0 = 10 – 40$ MJ/kg) as its flow rate is up to $G = 4$ g/s and total pressure is up to $P_0 = 50$ kPa (0.5 bar). The main parameters of the heater operation in the wind tunnel VAT-104 are studied by contact and optical diagnostic techniques. It is founded that the vibration and rotational temperatures in the settling chamber coincide within the experimental error limits (10%).
The results of heat flux measurements made with calorimeters and sensors with coatings of extremely high and extremely low catalytic activity enabled to establish that as the anode voltage was $U = 8.5 – 10.5$ kV and the pressure in the heater was $P_0 = (10 – 40)$ kPa,

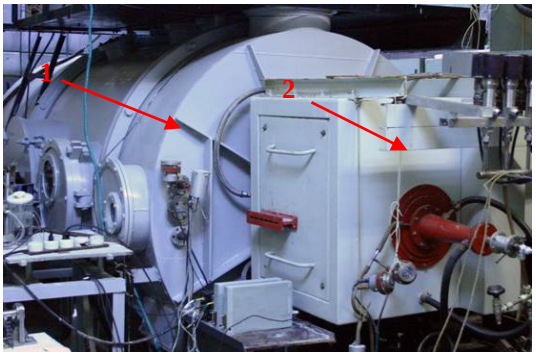

a). Photograph
1-working chamber, 2- high-frequency (HF) inductive heater

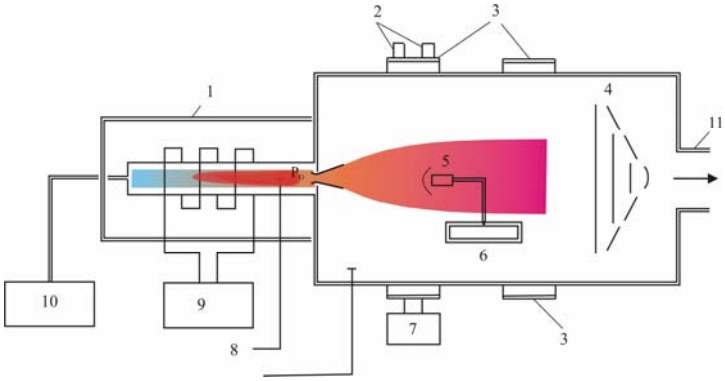

b). The basic schematic
1 - induction heater, 2 - CCD camera, 3 - optical windows, 4 - cooler, 5 - model, 6 - input mechanism, 7 – AGA thermo vision, 8 - pressure gauges, 9 - HF generator, 10 - gas supply, 11 – to the vacuum system

Figure 1. WT VAT-104

– the flow enthalpy is $i_0 = 10 – 40$ MJ/kg
– air dissociation degree is $\alpha = 0.5 – 0.9$;
– the power transferred to the working gas flow from the heater is $W_f \approx 50$ kW.
With the lower heater power, lower flow parameters can be realized: the pressure of $P_0 = 3 – 6$ kPa, $i_0 = 10 – 20$ MJ/kg, $\alpha = 0.1 – 0.3$.
The working cell is an Eifel chamber. It is a cylinder with the diameter of 1.6 m and length of 4 m. The inductive heater with a water-cooled nozzle is connected to the front end face of the working chamber. The back end face is connected to the vacuum capacity via a vacuum lock.
Inside the working cell, there is a fast-acting mechanism of model introduction into the flow and a heat exchanger which cools down the high-temperature gas jet after model immersed in flow. The model was introduced into the flow as the assigned stationary flow mode was reached in the wind tunnel, figure 2.

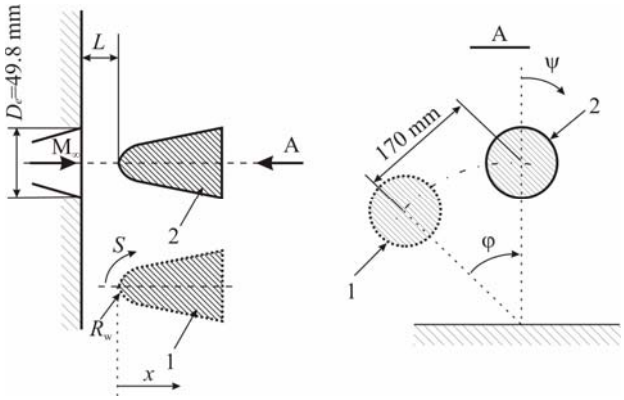

Figure 2. The fast-acting input mechanism.
1 - before model introduction into the flow, 2 – after model introduction

In this research, the Laval nozzle was utilized; it had the critical section radius $R^* = 7.5$ mm, outlet section radius $R_e = 24.9$ mm, and half angle in the supersonic part of 15º. The pressure in the working part of VAT-104 may vary from 1 to 1,000 Pa regarding the quantity and type of involved pumps and gas flow rates. In these experiments, the jet flowing out from the nozzle of VAT-104 is underexpanded. Mach numbers M = 4 – 8 can be reached in the jet at various distances from the nozzle cut.
Maximum duration of the test in VAT-104 is limited by the possibility of working chamber cooling; it varies from 20 minutes as the pressure in the settling chamber is $P_0 \approx 50$ kPa to two hours at $P_0 \approx 5$ kPa. The heat flux to the cold wall ($T_w = 18$ °C) in the critical point of the flat end face of the lengthwise-flowed cylinder with the radius of $R = 35$ mm is $q_0 = 100 – 1500$ kW/m^2, and the radiation-equilibrium temperature of the surface may reach $T_r = 1750$ °C.

Deviations of the enthalpy from one test to another normally do not exceed 3%. In repetitive tests, the error of heat flux determination is 5 – 10%.

2.2 Model

The methodical model purposed for the distribution of the heat flux density is made of stainless steel and has a shape of a blunt cone which is identical to the standard sample shape. The photo of the model is given in Figure 3.

Figure 3. The model photograph

There are 9 calorimetric heat-flux gages on the model; they are equipped with thermo-anisotropic bushings and a thermocouple to measure the temperature of their cold junction. Location of the heat flux probes is shown on Figure 3 and 4.

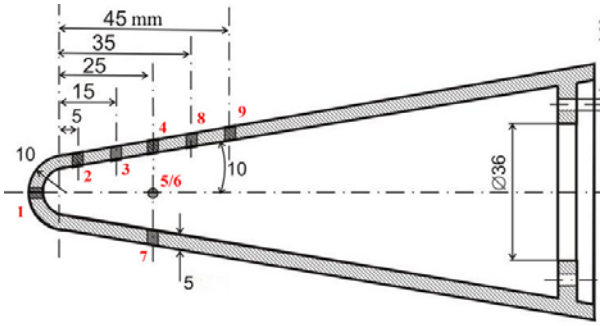

Figure 4. Location of the heat flux probes

Table 1: Location of the heat flux probes

Probe number	1	2	3	4	5	6	7	8	9
x, mm	0	15	25	35	35	35	35	45	55
S, mm	0.00	20.8	30.9	41.1	41.1	41.1	41.1	51.2	61.4
ψ, deg	0	0	0	0	270	90	180	0	0

The heat flux probe has a brass calorimeter shaped as a small cylinder, its diameter is 1.5 mm, length 4 mm. Thermo-electrode consists wires of “chromel” and “copel”, diameter 0.1 mm, which are welded to the back side of the cylinder (dot welding). All thermocouple cables are connected to the connector which is located in the aft body of the model.

A heat-insulating bushing, which presents a tight spiral of brass foil and a thin glass-cloth band, serves for thermal insulation of the calorimeter from the model walls. Spiral turns are glued with a high-temperature glue VK-21 (heat resistance up to 700 – 800°C). Owing to such a probe design, the temperature distribution by the cylinder depth and long turns of the brass foil are approximately similar (especially on the spiral turns adjoining to the calorimeter), figure 5.

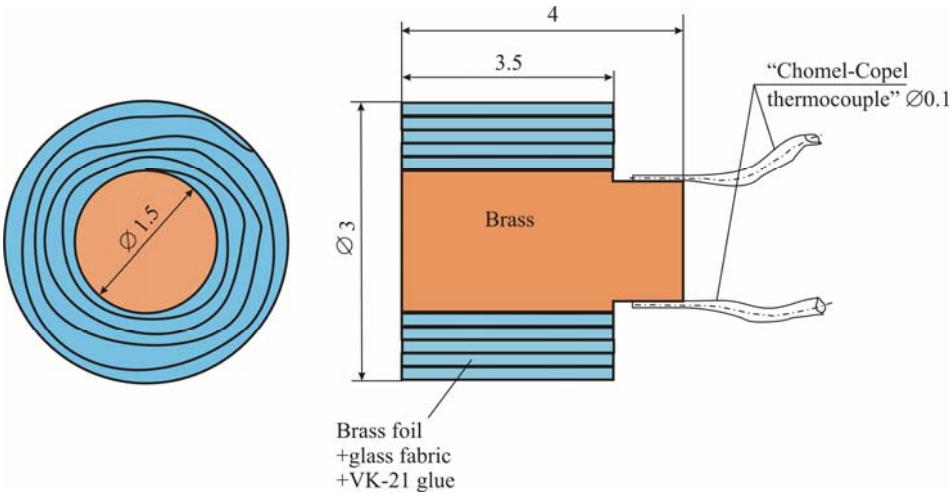

Figure 5. The heat flux probe design

At the same time, effective thermal conductivity across the spiral turns is not high because of the low thermal conductivity of the glass cloth and glue. It permits to linearize probe's characteristics and hence increase the potential measurement time up to 3 – 4 seconds. In order to sufficiently reduce leakages resulting from plasma flow, the probes were coated with an insulator (thin, approximately 2 μkm layer of gel SiO_2). It enabled us to illuminate discharge current to the gages and obtain more "pure" signals, whereas the influence of the SiO_2 layer on K_1 was insignificant.

Each heat-flux probe was graduated many times in pulse thermal calibrating facility ITGU NIO-8 TsAGI. The facility permits to supply step-function signals q_0 of the convective heat flux with known magnitudes. The probe calibrating factor K_1 is determined by the response signal $U_0(\tau)$.

$$K_1 = q/(dU/d\tau)$$

Later, these calibrating factors will be utilized to determine the heat flux density during the tests of the model in the WT VAT-104.

$$q = k\times(dU/d\tau), \text{ where } k = K_1\times K_2$$

here U is the probe signal in millivolts recorded during the tests, K_2 – the factor of the amplifier of the signals established in the WT VAT-104.

The model for pressure distribution measurement was equipped with 5 small-scale inductive gages (type DMI-0.6-III) for the rated range of 0.6 kgs/cm^2. The probes were preliminary mounted on a special unit installed inside the model body. Figure 6 presents the photo of the model with the probes inside.

Figure 6. The model for pressure distribution measurement

Receiving orifices of the gages (d_{in} = 1 mm) lied on one line along the model generatrix. The coordinates of pressure sampling points are shown on table 2.

Table 2: Orifices location

Probe number	1	2	3	4	5
x, mm	0	15	25	35	55
S, mm	0.00	20.8	30.9	41.1	61.4

Pedestal areas of the gages are connected with a sealed channel; this channel is a carrying collector for every gage, it has a special outlet tube, which connects the collector and working part of the wind tunnel and also serves as a channel of bearing pressure supply for gages calibration. Electrical leads of the gages are unsoldered for the connector RS32 TV. The gages work together with the amplifying apparatus on the carrier frequency 8ANCh-23. Magnetic biasing frequency for the probes is 20 kHz.
The gage at S =0 purposed for the measurement of the pressure in the critical point of the model has special thermal protection – a plug which presents a tangle of copper wire of 0.08 mm located in the channel of the receiving duct of the gage.

3. Results of numerical investigations of the flow around the model

Numerical simulation of the stationary laminar flow of the air plasma in the heater for experimental conditions in the WT VAT-104 TsAGI was performed on the base of full Navier-Stokes equations and simplified Maxwell equations for the time-averaged amplitude of the tangential component of the high-frequency electric field intensity $\vec{E}(t,x,r) = \vec{E}_\theta(x,r)e^{-i\omega t}$, written in the cylindrical system of coordinates, with due regard to the axial symmetry of the task. Here $\omega = 2\pi f$ is the circular frequency. Plasma radiation was ignored. The electromagnetic field is a superposition of the induction coil field поле and annular plasma currents; it was treated as a monochromatic one, with the assigned frequency f which depends on the high-frequency current in the inductor. For the calculation, the real inductor was replaced by four infinitely thin ring turns. The geometry of the discharge channel and inductor is shown in Figure 3.1.
The source terms (the Loren's force and Joule heat release) involved in the Navier -Stokes equations were expressed via the tangential component of the complex amplitude of the curl electric field.
The calculation of the high-frequency electromagnetic field was conducted together with the calculation of the gas-dynamic equations on the base of the local-one approximation of the Maxwell equations. The followings assumptions were used:

- the plasma is quasi-neutral;
- magnetic permeability of the plasma is μ =1;
- dielectric permeability of the plasma does not depend on the electromagnetic field and hence does not depend on the coordinates;
- the bias current can be ignored;
- the variation of the electric field in the axial direction can be ignored as compared to its variation in the radial direction

$\frac{\partial}{\partial x} E_\theta << \frac{\partial}{\partial r} E_\theta$.

The latter assumption leads us to the locally-one approximation for the Maxwell equations, and it significantly simplifies the task. The corresponding equation for the definition of the tangential component of the curl electric field and boundary condition for this equation are given in [4-5] where the flow of the equilibrium air plasma was considered.
During the combined calculation of the flow and electromagnetic field in the heater of WT VAT-104 TsAGI, the power N_{pl} applied to the discharge was assigned as a governing parameter; the respective current in the inductor was determined during the solution process. In turn, the value of N_{pl} was found with the aid of the generator power N_{ap} measured experimentally, by the anode supply multiplied by the plasmatorch efficiency.
Figure. 7 and 8 presents the results of calculated distribution of the static temperature and Mach number respectively; the data illustrate the pattern of the flow around the blunt cone model at the static pressure of the flow in the output cross section of the nozzle; the pressure is somehow above the pressure in the working part of the wind tunnel.

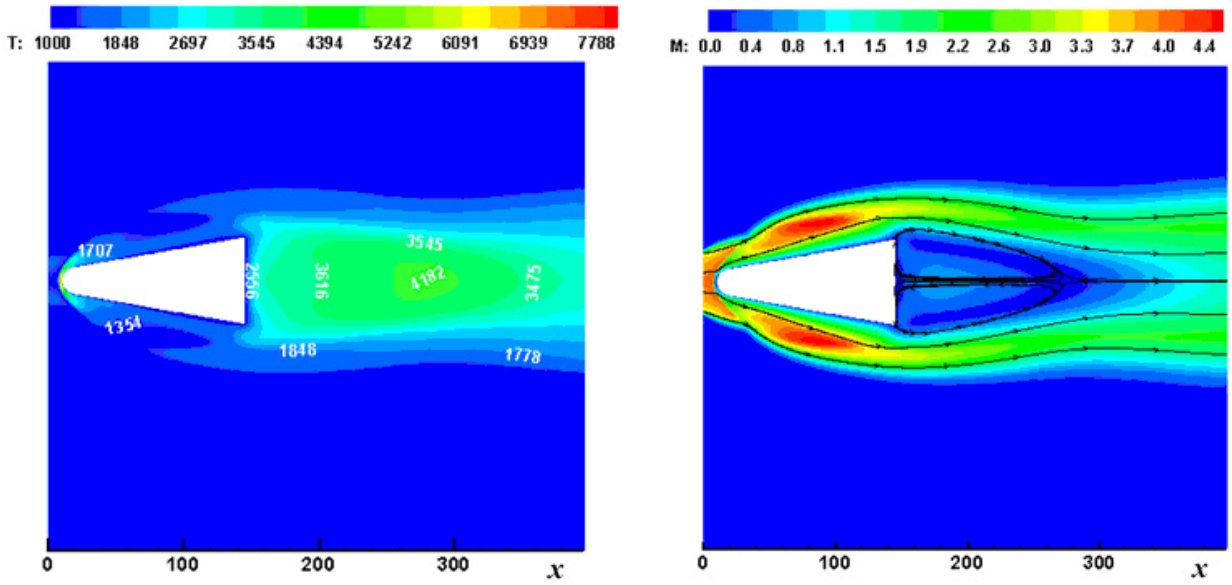

a) b)

Figure 7. The flow structure near the a blunt cone immersed in a supersonic flow
a) Static temperature, K; b) Mach Number

The pressure ratio on the cone surface P_w to the full pressure P_0 (in the heater) at the nose part of the model (at $S \le 80$ mm; inside the "Mach cone" of the underexpanded jet) don't depend from the working chamber pressure P_{wc} (fig. 8). At the same time, the pressure ratio on the model surface P_w to the full pressure P_0 decreases with the distance increase from the nozzle section exit to the stagnation point of the model $X_s = L$ (fig. 8 and 9). Specifically the pressure ratio in the critical point $S = 0$ (the stagnation pressure) P_s to the full pressure P_0 is changed sufficiently.

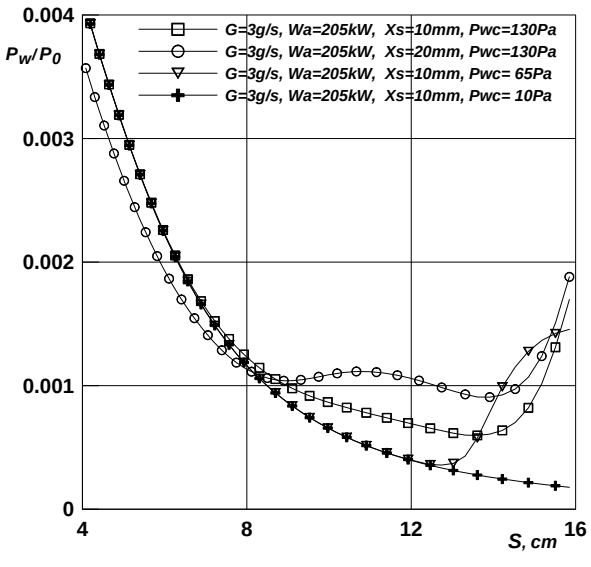

Figure 8. The dependences of the pressure ratio at the cone surface to the full pressure P_w/P_0 for various pressure values in the working chamber

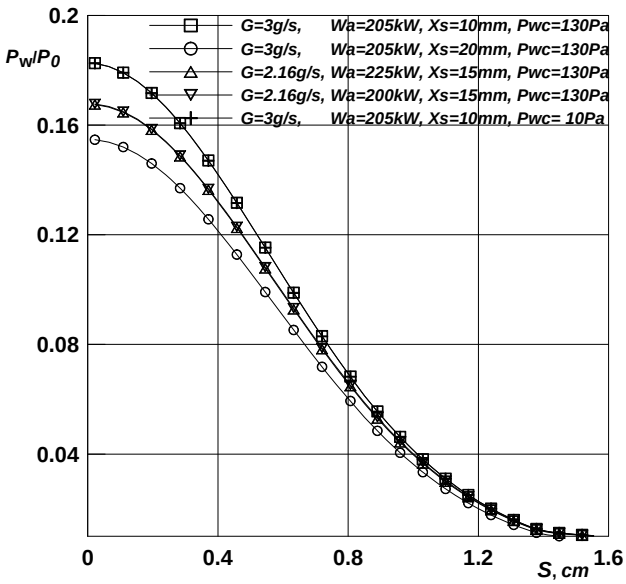

Figure 9. The dependences of the pressure ratio at the nose part of the model to the full pressure P_w/P_0 for various parameters.

4. Experimental investigation of the heat flux distribution and pressure over the model surface

The experiment sequence was the following: the model was installed on a holder fastened into a fast-acting mechanism of model introduction in the flow. Before being introduced into the flow, the model axis was parallel to the nozzle axis and 160 mm far from it, the critical point of the model was at the distance of X=10 mm from the nozzle output section.
Then the working part of the wind tunnel was sealed and pumped out. As the pressure of 1 – 100 Pa was reached, the plasmatorch generator was actuated. The discharge was ignited, and smooth mode onset was carried out via increased anode power of the heater W_a and air pressure ahead of the throttle (pressure in the settling chamber P_{fk}). The duration of the mode onset was about 50 – 80 s. As the necessary parameters (W_a and P_{fk}) were reached, the operator introduced the model in the flow. The heater was switched off in 2 – 3 s past introducing the model in the flow.

4.1 Heat flux distribution

As an example, let us consider the results of one of the tests, Figure 10. At this figure the dependence of the pressure in the settling chamber and anode power of the heater on time are presented. The pressure in the settling chamber was P_{fk} = 355 Torr (the pressure in the settling chamber P_{fk} practically does not differ from full pressure P_0), the heater power was W_a = 190 kW, air flow rate G = 2.5 g/s.

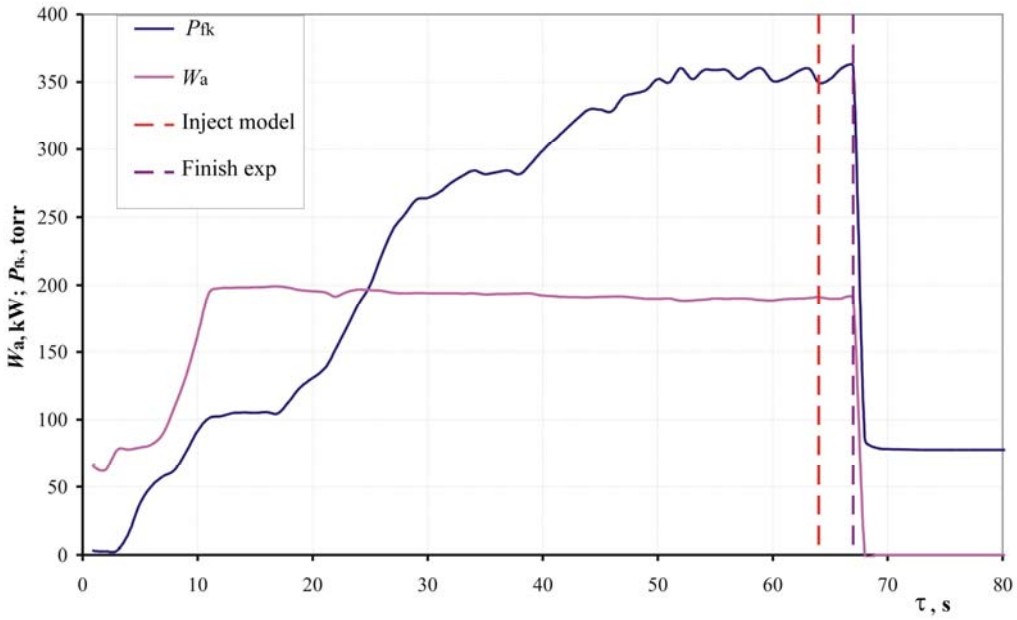

Figure 10. The dependence of the pressure in the settling chamber and anode power of the heater on time

The characteristic record of the thermocouple signals in U_i(mV) in time for every calorimeter for one of the tests are shown on figure 11.

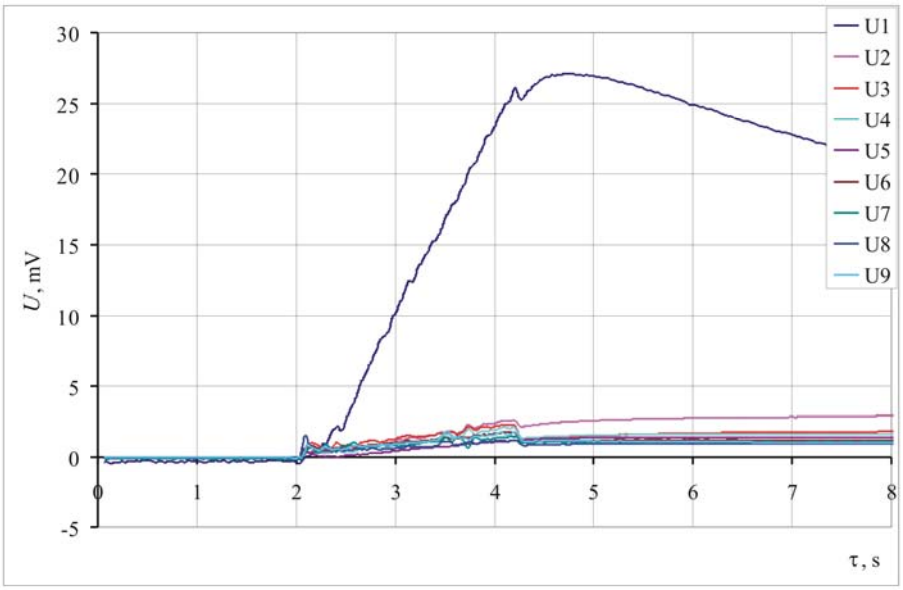

Figure 11. $U_i = f(\tau)$

Here, curves numbers correspond to the heat flux probes numbers (table 1).
The resulting graph of the heat flux distribution q_w over the model length is presented in Figure 12. The anode power of the heater in each run was $W_a = 195 \pm 5$ kW.

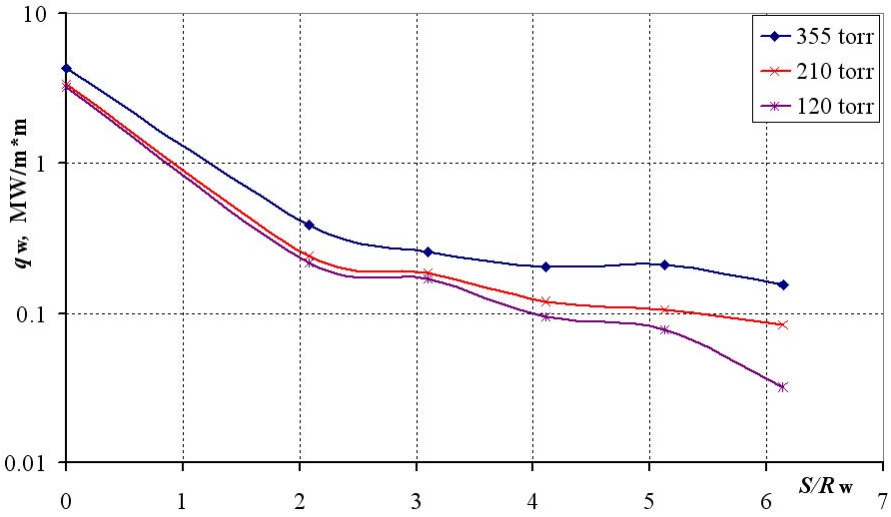

Figure 12. $q_w = f(S/R_w)$

It follows from Figure 13 that the obtained experimental findings and numerical data of the heat flux are in agreement (in the calculations, the ratio of the power applied to the gas flow to the anode power of the heater, as well as some other characteristics, were taken from the evaluations of the known values of similar wind tunnels. At the moment, investigations are performed to determine the needed characteristics of the WT VAT-104).

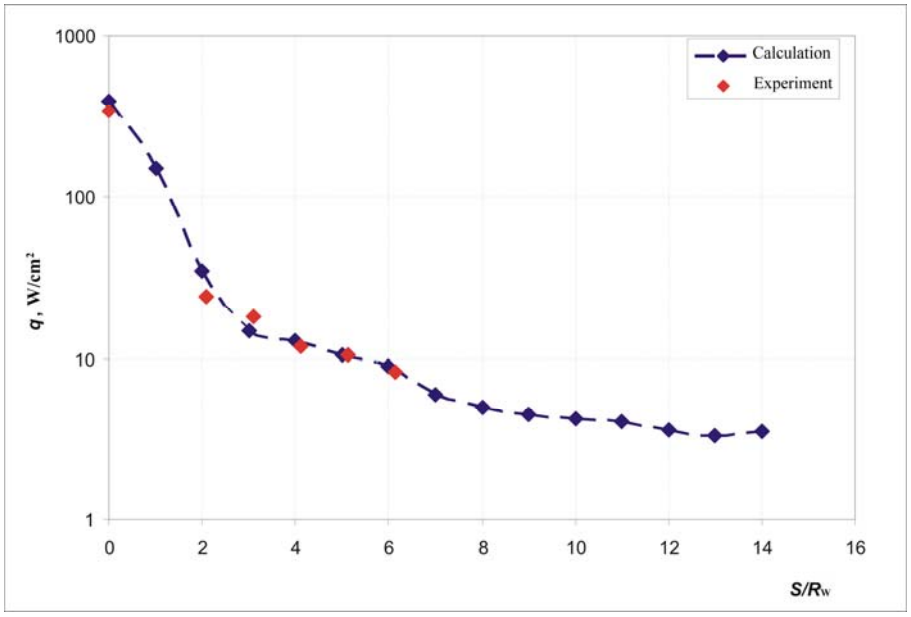

Figure 13. The heat flux distribution over the model surface.

4.1 Pressure distribution

In order to determine the pressure distribution, four tests were carried out at various pressure in the settling chamber and constant heater power.
Let us analyze the results of one test. The settling-chamber pressure was P_{fk} = 350 torr. Figure 14 presents the comparison of the pressure distribution versus the distance to the critical point (experimental value) with the numerical data. It is evident that the pressure obtained in the test is in good agreement with the results of numerical simulation.

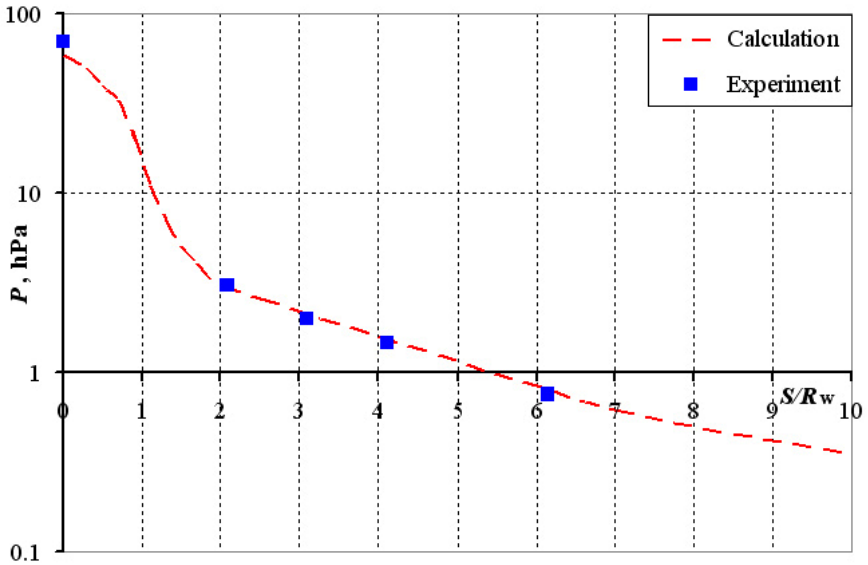

Figure 14. The pressure distribution over the model surface.

Conclusions

The numerical and experimental investigations were carried out to study the flow, heat flux distribution and pressure distribution over the front and side surfaces of the blunt cone which was in non-equilibrium high-enthalpy (h_0 = 25

MJ/kg) supersonic (M = 4) air flow. The tests were performed in the wind tunnel VAT-104 TsAGI. The nose part of the model with the small-radius nose $R_w = 10$ mm and half-angle $\theta = 10°$ was inside the "Mach cone of the underexpanded jet flowing out from the WT nozzle. Obtained numerical and experimental data are in qualitative agreement. These results permit to start respective investigations of various methods of the thermal protection of those bodies.

Acknowledgement

The authors are deeply indebted to colleagues: N.O. Mjatkovsky, S.M. Pokhvalinsky, A.A. Shamshurin, A.A. Trofimov, and Yu. V. Zhilin for the help at preparation, performance, and analysis of the results of this work.

This work was supported by the Russian Foundation for Basic Research (Grants No. 11-01-00882-a, 11-01-00111-a).

References

[1] Park C., Howe J.T., Jaffe R.L. and Candler G.V.,Review of Chemical-Kinetic Problems of Future NASA Missons. II: Mars Entries. 1994. *J.of Thermophysics and Heat Transfer, Vol.8, No.1, 1994*

[2] Afonina N., Cromov V., Sakharov V. 2004. HIGHTEMP technique for High Temperature Gas Flows Simulations. In: *European Space Agency (Special Publication) ESA SP 5th European Symposium on Aerothermodynamics for Space Vehicles. SP 563. ESA Publications Division Cologne ESTEC. Noordwijk. p. 119-123.*

[3] Sakharov V., Gromov V. 2004. CFD modeling of thermally and chemically nonequilibrium flows in discharge channel and in under-expanded plasmatron jets over a butt-end probe. In: *European Space Agency (Special Publication) ESA SP 5th European Symposium on Aerothermodynamics for Space Vehicles. SP 563. ESA Publications Division Cologne ESTEC. Noordwijk. p. 323-328.*

[4] Sakharov V.I. 2007. Numerical simulation of thermally and chemically nonequilibrium flows and heat transfer in underexpanded induction plasmatron jets. *J. Fluid Dynamics. Maik Nauka/Interperiodica Publishing (Russian Federation). V. 42. N 6. p.1007-1016.*

[5] Sakharov V.I. 2007. Separation of chemical elements in the discharge channel of an inductive plasma gun. *J. Fluid Dynamics. Maik Nauk./Interperiodica Publishing (Russian Federation). V. 45. N 4. p. 647-655.*

[6] Vasil'evskii. S.A., Kolesnikov. A.F. 2000. Numerical Simulation of Equilibrium Induction Plasma Flows in a Cylindrical Plasmatron Channel. *J. Fluid Dynamics. Maik Nauka/Interperiodica Publishing (Russian Federation). V. 35. N 5. p.769-777.*

[7] B.E. Zhestkov. V.V. Shvedchenko. 1996. Evaluation of Material Oxidation in Induction Plasmatron under Simulated Re-entry Conditions. In: *ESA-WPP-103. p.204-215.*

[8] B.E. Zhestkov. D.V. Ivanov. V.V. Shvedchenko. I.V. Jegorov. W.P.P. Fischer. and J. Antonenko. 1999. Calculated and experimental flat and wavy surface temperature distributions. In: *AIAA paper 99-0733.*

[9] B.E. Zhestkov. V.S. Terent'eva. 2010. Multifunctional Coating MAI D5 Intended for the Protection of Refractory Materials. *J. Russian Metallurgy. Vol. No. 1. pp. 33-40. Pleiades Publishing. Ltd.*

[10] Borovoy V.Ya., Egorov I.V., Skuratov A.S., Paderin L.Ya., Shtapov V.V., Vaganov A.V., Vasilevskiy E.B., B.E. Zhestkov. 2011. Experimental researches in high temperature facilities of TsAGI. In: *4th European conference for aerospase sciencies. Peterburg. CD. 1184-1859-1DR. id 602.*